Optimal electromechanical control of the excitonic fine structures of droplet epitaxial quantum dots

Shun-Jen Cheng,* Yi Yang,† Yu-Nien Wu, Yu-Huai Liao, and Guan-Hao Peng
Department of Electrophysics, National Chiao Tung University, Hsinchu 300, Taiwan, Republic of China

(Received 31 August 2018; revised manuscript received 2 October 2018; published 19 October 2018)

The intrinsic fine structure splittings (FSSs) of the exciton states of semiconductor quantum dots (QDs) are known to be the major obstacle for realizing the QD-based entangled photon pair emitters. In this paper, we present a theoretical and computational investigation of the excitonic fine structures of droplet-epitaxial (DE) GaAs/AlGaAs QDs under the electromechanical control of micromachined piezoelectric actuators. From the group theory analysis with numerical confirmation based on the developed exciton theory, we reveal the general principle for the optimal design of micromachined actuators whose application onto an elongated QD can certainly suppress its FSS. We show that the use of two independent tuning stresses is sufficient to achieve the FSS elimination but is not always necessary as widely deemed. The use of a single tuning stress to eliminate the FSS of an elongated QD is possible as long as the crystal structure of the actuator material is in coincidence with that of the QD. As a feasible example, we show that a *single* symmetric biaxial stress naturally generated from the (001) $[Pb(Mg_{1/3}Nb_{2/3})O_3]_{0.72}-[PbTiO_3]_{0.28}$ (PMN-PT) actuator can be used as a single tuning knob to make the full FSSelimination for elongated DE GaAs QDs.

DOI: 10.1103/PhysRevB.98.155315

I. INTRODUCTION

Generation of polarization-entangled photon pairs is a vital element in advanced quantum photonic applications, such as quantum cryptography and quantum teleportation [1]. Semiconductor quantum dots (QDs) were predicted to be a promising nanomaterial for being "on-demand" entangled photon pair emitters (EPPEs), which are key devices necessary in quantum cryptography and quantum teleportation [2–5]. However, in reality photo-excited QDs usually fail to generate such polarization-entangled photon pairs because of the intrinsic fine structure splitting (FSS) between the single bright-exciton (BX) doublet as the intermediate states in the process of spontaneous biexciton-exciton-vacuum cascade decay. The FSS of an exciton in a self-assembled QD is caused by the electron-hole (*e*-*h*) exchange interactions, which are likely induced by any slight symmetry breaking of QD structures, such as shape elongation, strain, or composition randomness, and leads to the destruction of entanglement with the reveal of the which-path information in the processes of spontaneous exciton decay [6]. Thus, technologies for fully eliminating the exciton FSS, against the inherent or extrinsic symmetry breaking of QDs have been desired for a long time and are still under active development for QD-based photonic applications [7–10].

In earlier times, most experiments attempted to use single generic fields, e.g., electrical [7,11,12], magnetic [13,14], optical [15], or stress fields [16], as *single* tuning knobs to suppress the FSSs of QDs, but the yield of successful devices was extremely low. As a known example, the FSSs of QDs can be well tuned by a single uniaxial stress but hardly really tuned to be zero [16,17].

Until some years ago, a conceptual and technological breakthrough was first proposed and experimentally confirmed by Trotta *et al.* to solve the problem [9]. They show that at least *two* tuning knobs are needed for a thorough elimination of the FSSs of QDs [9,18,19]. In the experiment, with the simultaneous application of a uniaxial stress and vertical electrical bias, the FSSs of the inherently strained InAs/AlGaAs QDs were fully eliminated in a universal and deterministic manner. Years later, with the advances in the fabrication of micromachined actuators, the deterministic generation of entangled photon pairs from InAs/AlGaAs QDs was also realized by means of simultaneously applying two independently tuned uniaxial stresses onto the QDs [20]. The realization of the QD-based EPPEs by means of the electromechanical control opens up a prospect of the integration of QD-based photonics with microelectromechanical systems (MEMSs). Inspired by the progress, currently more attempts are devoted to developing the versatile QD-based EPPEs with the functionalities useful in scalable integrated photonic systems [20–22]. In a sense, the need and use of two tuning knobs for the FSS tuning hinder the versatility of devices that also require additional tuning knobs for the functional operations [23]. Thus, for practical applications and also fundamental curiosity, the following questions arise: Why are two tuning knobs necessary and can the number of required tuning knobs be reduced?

In this paper, we present a theoretical and computational investigation of the excitonic fine structures of inherently unstrained GaAs/AlGaAs droplet-epitaxial QDs (DE-QDs) under the electromechanical control, implemented by micromachined $[Pb(Mg_{1/3}Nb_{2/3})O_3]_{0.72}-[PbTiO_3]_{0.28}$ (PMN-PT) piezoelectric actuators in multilegged structures [21,24–26]. As compared with more extensively studied InAs/AlGaAs QDs grown in the Stranski-Krastanov (SK) mode [27,28], GaAs QDs grown by DE technique are advantageous in the well-controlled shape geometry [29,30], negligible interdiffusion at interfaces [31], and the absence of internal strain [32]. Notably, the absence of inherent strain makes the electronic

*Corresponding author: sjcheng@mail.nctu.edu.tw
†Corresponding author: yiyang@mail.nctu.edu.tw

and excitonic structures of GaAs DE-QDs sensitive to and highly tunable by external stress [26,33–35].

From the group theory analysis with numerical confirmation based on the multiband exciton theory, we derive explicitly the general principle for the optimal arrangement of uniaxial stresses from micromachined PMN-PT actuators that can certainly suppress the FSSs of elongated GaAs DE-QDs fully. The principle to follow is that a full elimination of the FSS, tuned by external knobs, of an elongated QD can always be possible as long as the symmetry of the QD can be kept invariant during the tuning process. Surprisingly, we find that that, beyond common intuitive understanding, the use of two tuning knobs is actually a sufficient but not a necessary condition for a deterministic elimination of the FSS of an elongated QD. As a feasible example, it is shown that a *single* symmetric biaxial stress naturally generated from the (001) PMN-PT actuator [35–37] can be used as a single tuning knob to make the full FSS elimination, and advantageous in the robustness of the FSS tuning against the poorly controlled orientation variations of actuators. The deterministic elimination of the FSSs of zinc-blende GaAs QDs by using a single symmetric biaxial stress from (001) PMN-PT actuator is achievable by taking advantage of the compatibility of crystal symmetry between the QD- and piezoelectric actuator materials and essentially related to the stress-enhanced valence band mixing (VBM) in the QD-confined exciton [38].

This paper is organized as follows. The next section presents the theoretical and computation methodology used throughout this paper. In Sec. II A, we present the group theory analysis for the excitonic fine structures of elongated semiconductor QDs under the action of generic tuning stresses. Section II B is devoted to the theory of electron-hole exchange interaction in a QD-confined exciton and the numerical implementation for the simulation of the fine structures of stressed GaAs/AlGaAs QDs. In Sec. III, we discuss the predicted excitonic fine structures of stress-controlled QDs by the group theory. Then, we present a general principle for the optimal design of the stress actuators predicted from the analysis, with confirmation by the numerical computation. In Sec. IV, we establish a valid simplified exciton model that incorporates the nonlinear effect of the biaxial stress and valence-band-mixed nature of exciton. Finally, we conduct the model analysis to discuss several advantageous features of the zinc-blende QDs controlled by a single symmetric biaxial stress. Section V concludes this work.

II. THEORETICAL AND COMPUTATIONAL METHODS

A. Group theory analysis

We begin with the group theory analysis for a single exciton in an elongated QD made of zinc-blende T_d semiconductor. Figure 1 depicts a GaAs QD in the shape of C_{2v} symmetry mounted on a PMN-PT piezoelectric crystal and stretched by the generated stresses. Below we summarize the main predicted features of exciton fine structures of the QDs under the stress control. The technical details of the analysis are given in Sec. S1 of Supplemental Material [39].

1. Bulk

Disregarding the C_{2v} quantum confinement of QD, the states of a spin exciton in a T_d crystal that are created from the direct product of the conduction band and the valence band states are known as $\Gamma_{6c} \times \Gamma_{8v} = \Gamma_{3X} + \Gamma_{4X} + \Gamma_{5X}$ [17], which consists of a doublet in the irreducible representation (irrep) Γ_{3X} and two triplets in Γ_{4X} and Γ_{5X}. The exciton states in the irrep Γ_{5X} (Γ_{3X} and Γ_{4X}) are optically active (inactive) and referred to as the BX [dark exciton (DX)] states, according to the Wigner-Eckart theorem. Throughout this paper, we shall use the subscript indices c, v, X, and s to indicate conduct band, valence band, exciton state, and spin, respectively.

2. C_{2v} QDs

With the C_{2v} quantum confinement of QD, the degeneracy of the BX states in the triplet irrep Γ_{5X} is lifted. With the addition of spin-orbit interaction, the conduction band turns out to be a doublet irrep $\Gamma_{1c} \times \Gamma_{5s} = \Gamma_{5c}$, and the topmost valence bands Γ_{2v} and Γ_{4v} are regrouped into the doublet irreps $\Gamma_{2v} \times \Gamma_{5s} \equiv \Gamma_{5v}^{(2)}$ is referred to as the heavy hole (HH), and $\Gamma_{4v} \times \Gamma_{5s} \equiv \Gamma_{5v}^{(4)}$ is referred to as the light hole (LH) [17].

Since both of the HH and LH bands belong to the same doublet irreps Γ_{5v}, it is natural to consider $\Gamma'_{5v} = \Gamma_{5v}^{(2)} + \tilde{\beta}_{\rm HL}\Gamma_{5v}^{(4)}$ for the valence-band-mixed hole states where the HH and LH components are intrinsically mixed. Here, we introduce the complex coefficient $\tilde{\beta}_{\rm HL} \equiv \beta_{\rm HL}e^{-i\phi_\beta}$ to parametrize the degree as well as the phase of VBM that are essentially associated with the symmetry of system. For a C_{2v} QD, $\Gamma_{5v}^{(2)}$ and $\Gamma_{5v}^{(4)}$ should keep invariant under the action of the symmetry transformations for C_{2v} (C_{2z}, σ_y, σ_x,...) as given in the character table of Fig. 2(a), so do Γ'_{5v}. Note that, with arbitrary value of $\tilde{\beta}_{\rm HL}$ the mixture of HH and LH, $\Gamma'_{5v} = \Gamma_{5v}^{(2)} + \tilde{\beta}_{\rm HL}\Gamma_{5v}^{(4)}$, might not belong to the representation of C_{2v} if the chosen phase angle ϕ_β is improper. In fact, only the phase angles, $\phi_\beta = 0$ or π, can match the corresponding symmetry transformations of C_{2v}, and indicates the real value of $\tilde{\beta}_{\rm HL}$. A real $\tilde{\beta}_{\rm HL}$ indicates the fixed relative phase between the HH and LH components and the fixed orientation of the resulting optical polarizations. Remarkably, the invariance of optical orientation of a single exciton in a QD under the tuning of external fields has been well recognized as a crucial signature to the feasibility of tuning the FSS of the QD down to zero, as will be discussed more later [9,18,22,23,33].

3. Effects of valence band mixing

With the VBM nature, the states of the exciton bound by electron-hole Coulomb interactions are created from the direct product of the Γ_{5c} conduction band and the Γ'_{5v} valence band becomes $\Gamma_{5c} \times \Gamma'_{5v} = \Gamma_{1X} + \Gamma_{2X} + \Gamma_{3X} + \Gamma_{4X}$, composed of the DX singlet belonging to Γ_{3X} and the BX triplet belonging to Γ_{1X}, Γ_{2X} and Γ_{4X}, optically polarized along the z, x, and y, respectively. The character table for the spin double group of C_{2v} is presented in Fig. 2(a). In this work, we are mainly interested in the x- and y-polarized BX doublet (Γ_{2X} and Γ_{4X}) that can emit light vertically out of the QDs grown on the (001) substrate.

In principle, the four exciton states (Γ_{1X}, ..., Γ_{4X}) of a C_{2v} QD that belong to the different irreducible representations should own distinctive energies and are subject to level splittings, except that some accidental degeneracy happens. Thus,

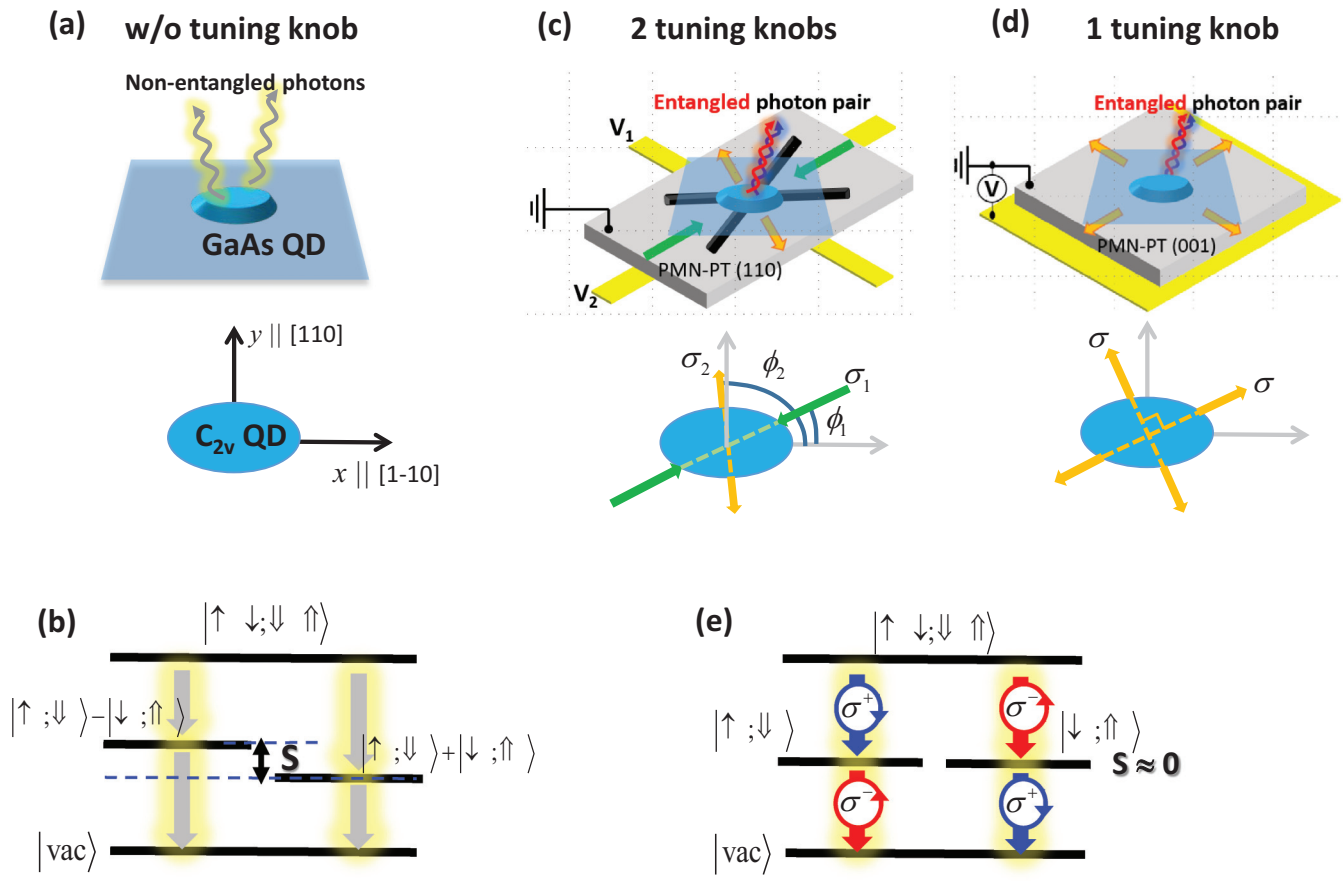

FIG. 1. Schematics of (a) a photo-excited QD in the elongated shape of C_{2v} symmetry that successively emits a pair of photons not in entanglement, and, correspondingly, (b) the biexciton and single exciton levels of the elongated QD, with a nonzero fine structure splitting ($S \neq 0$) between the single-exciton doublet. (c) A C_{2v} QD with two mechanical tuning knobs, a set of two uniaxial stresses generated and controlled by a (110) micromachined PMN-PT actuator. Generation of polarization-entangled photon pairs from the stressed QD is possible if the strengths, (σ_1, σ_2), and the orientations, (ϕ_1, ϕ_2), of the two tuning uniaxial stresses are chosen appropriately. (d) The C_{2v} QD with a single tuning knob of symmetric biaxial stress from (001) PMN-PT crystal that can emit a pair of photons in entanglement with only appropriate adjustment of the strength of the single stress, irrelevant to the orientation of the stress axes. (e) The exciton-level schematics of the QD that can emit entangled photon pairs, where the fine structure splitting (S) is intrinsically zero or eliminated by external tuning knobs.

the only possibility of crossing over the Γ_{2X} and Γ_{4X} BX levels of a C_{2v} QD is by means of the *accidental degeneracy* that might be made by using some external tuning knobs. As pointed out previously by Singh and Bester in Ref. [17], the formation of such an accidental degeneracy of the BX doublet of an asymmetric QD could be possible *if and only if* the BX states belong to different irreducible representations. From our analysis, it is shown that, as long as C_{2v} symmetry of QD can be preserved during the FSS-tuning, the BX doublets surely stay in the different irreps Γ_2 and Γ_4 [see Figs. 2(a) and 2(c) for illustration].

4. *Effects of external tuning knobs*

Yet, in reality, imposing tuning knobs onto a QD to tune the FSS is likely to break the C_{2v} symmetry down to the lower ones, say C_2 symmetry. For a QD in the low symmetry caused by knob tunings, it turns out that the four exciton states belong to the irrep $2\Gamma_{1X} + 2\Gamma_{2X}$ in the C_2 group (see Fig. 2(b) for the character table) with the two BX singlets optically polarized along the x and y directions belonging to the same irrep Γ_{2X}, and it becomes impossible to eliminate the FSS of the QD in any way. Figure 2(d) depicts the exciton levels of a QD in the lowest C_2 symmetry, which are always anticrossed and cannot recover the degeneracy by knob tunings. The same conclusion can be obtained also for the even lower C_1 symmetry in which only one representation exists. In the situation of the low symmetry, it is thus necessary to use the second tuning knob to retain the C_{2v} symmetry and the possibility of eliminating the FSS. This accounts for that the successful elimination of the FSSs of QDs usually relies on the use of two tuning knobs, e.g., the combination of two independently controlled stresses, or that of a stress and an electric field [9,18,20].

Remarkably, with the recent advances in the micromachine techniques, the PMN-PT actuators can be fabricated in the multilegged structures to generate multiple (N) stresses (acting as mechanical tuning knobs), allowing for more flexible controls and additional functionalities of devices. Recently, the micromachined piezoelectric actuators in the three-legged, four-legged, and six-legged structures have been demonstrated for a full control of the generated in-plane stress tensor in semiconductor nanomembranes [20–22,35]. With the

(a)

The character table of the spin double group C_{2v}

C_{2v}	E	C_2	σ_y	σ_x	*Basis function*
Γ_1	1	1	1	1	z
Γ_2	1	-1	1	-1	x
Γ_3	1	1	-1	-1	xy
Γ_4	1	-1	-1	1	y
Γ_5	2	0	0	0	

(b)

The character table of group C_2

C_1	E	C_2	*Basis function*
Γ_1	1	1	z
Γ_2	1	-1	x, y
Γ_3	2	0	

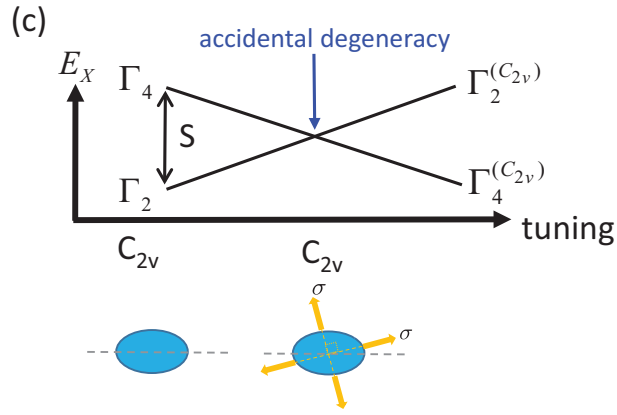

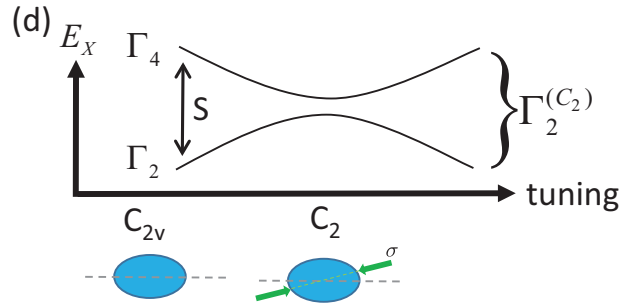

FIG. 2. The character tables of (a) the spin double group C_{2v} and (b) group C_2. (c) Schematics of the stress-tuned exciton levels of a C_{2v} QD with the preservation of the C_{2v} symmetry, e.g., by means of symmetric biaxial stress. In this case, a direct crossing (leading to $S = 0$) of the distinct exciton levels belonging to different irreducible representations, Γ_2 and Γ_4, can be made by an accidental degeneracy. (d) Schematics of the exciton levels of an elongated C_{2v} QD whose symmetry is reduced to C_2 by a misaligned uniaxial stress from the elongation axis. Without the preservation of the C_{2v} symmetry, the two exciton states belong to the same irreducible representations, Γ_2, and no level crossing can happen.

multilegged structure, the total generated stress is composed of multiple stresses each of which can be individually controlled and serves as an independent tuning knob. With the multiple tuning stresses, the EPPE devices that are wavelength tunable and suited for being quantum repeaters have been successfully fabricated, where two stresses are used for the suppression of the FSS and the others for the tuning of the light wavelength or other functionalities [20,21].

B. Deterministic elimination of exciton FSS by N uniaxial stresses

The resultant strain in a GaAs QD under N uniaxial stresses with the magnitudes $\{\sigma_i\}$ and the angles with respect to the elongation-axis $\{\phi_i\}$ is derived, through the standard procedures of tensor transformation as detailed in Sec. S2 of Ref. [39], as characterized by the nonzero strain tensor elements given by

$$\epsilon_{xx} = \frac{s_{11}+s_{12}}{2}\cdot\left(\sum_{i=1}^{N}\sigma_i\right) + \frac{s_{44}}{4}\cdot\left(\sum_{i=1}^{N}\sigma_i\cos 2\phi_i\right),$$

$$\epsilon_{yy} = \frac{s_{11}+s_{12}}{2}\cdot\left(\sum_{i=1}^{N}\sigma_i\right) - \frac{s_{44}}{4}\cdot\left(\sum_{i=1}^{N}\sigma_i\cos 2\phi_i\right),$$

$$\epsilon_{xy} = \frac{s_{11}-s_{12}}{2}\cdot\left(\sum_{i=1}^{N}\sigma_i\sin 2\phi_i\right),$$

$$\epsilon_{zz} = (s_{11}+s_{12})\cdot\left(\sum_{i=1}^{N}\sigma_i\right), \tag{1}$$

where the elastic compliance constants are $s_{11} = 0.0082\,\mathrm{GPa}^{-1}$, $s_{12} = -0.002\,\mathrm{GPa}^{-1}$, and $s_{44} = 0.0168\,\mathrm{GPa}^{-1}$ for GaAs [40].

Following the Neumann's principle [41,42], the strain tensor given by Eqs. (1) owns the C_{2v} symmetry if it is invariant under the operation of any C_{2v} symmetry operators. As detailed in Sec. S2.D of Ref. [39], one can show that the strain generated by N tuning uniaxial stresses can keep invariant the symmetry of C_{2v} and enables the full FSS elimination for a C_{2v} QD as long as the following equation for the arrangement of the stresses is fulfilled:

$$\sum_{i=1}^{N}\sigma_i\sin 2\phi_i = 0. \tag{2}$$

Equation (2) can serve as a general guideline for the optimal design of the useful micromachined actuators that can generate N uniaxial stresses for the deterministic control and

elimination of the FSSs of elongated QDs. Without losing the generality, hereafter we shall focus the study on the QDs under single-stress ($N = 1$) or dual-stress ($N = 2$) controls, which are most feasible to be implemented in experiments [35].

C. Numerical approaches

To confirm the prediction of the group theory analysis, we carry out the numerical calculations of the spectral fine structures and optical polarizations of single excitons in GaAs DE-QDs under various single- and dual-stress controls by using the computational methodology employed in Refs. [43–46]. Considering the GaAs material as a wide band-gapped semiconductor, we neglect the weak coupling between the conduction and valence bands, and compute separately the electronic structures of an electron and a valence hole in a GaAs QD in the single-band theory and the four-band $k \cdot p$ theory, respectively. In the former (latter) theory, the wave function of a conduction electron (a valence hole) in a QD is written as $\psi^e_{i_e}(\vec{r}) = g^e_{i_e}(\vec{r})u^c_{s_z}$ ($\psi^h_{i_h}(\vec{r}) = \sum_{j_z=\pm1/2,\pm3/2} g^h_{i_h}(\vec{r})u^v_{j,j_z}$), where $g^{e/h}_i$ are the slowly varying electron/hole envelope functions, $i_{e/h}$ stands for a composite index composed of those of the orbital and spin of an electron/a hole state, s_z is the z component of electron spin, j_z is the z component of the angular momentum $j = 3/2$ of valence hole, and $u^c_{s_z}$ ($u^v_{j=3/2,j_z}$) is the microscopic periodic part of the Bloch function of the conduction (valence) band. Based on the calculated electronic structures of an electron and a valence hole in a GaAs QD, the theory for the electron-hole exchange interaction of an exciton in the QD is established and used to compute the excitonic fine structures.

1. Four-band $k \cdot p$ model for a valence hole in a stressed QD

In the four-band model, the Hamiltonian for a single hole in a stressed QD is formulated as a 4×4 matrix composed of the kinetic energy-, strain-, and potential parts, $H_h = H^h_k + H^h_\epsilon + V^h_{\rm QD}$. In the basis of the Bloch functions ordered by $\{u_{j,j_z}\} = \{|u_{\frac{3}{2},\frac{3}{2}}\rangle, |u_{\frac{3}{2},\frac{1}{2}}\rangle, |u_{\frac{3}{2},-\frac{1}{2}}\rangle, |u_{\frac{3}{2},-\frac{3}{2}}\rangle\}$, the Hamiltonian is expressed as [29,40,46,47]

$$H_h = \begin{pmatrix} P+Q & -S & R & 0 \\ -S^+ & P-Q & 0 & R \\ R^+ & 0 & P-Q & S \\ 0 & R^+ & S^+ & P+Q \end{pmatrix} + V^h_{\rm QD} I_{4\times4}\,, \tag{3}$$

where $P = P_k + P_\epsilon$, $Q = Q_k + Q_\epsilon$, $R = R_k + R_\epsilon$, $S = S_k + S_\epsilon$, $P_k = \frac{\hbar^2\gamma_1}{2m_0}(k_x^2 + k_y^2 + k_z^2)$, $Q_k = \frac{\hbar^2\gamma_2}{2m_0}(k_x^2 + k_y^2 - 2k_z^2)$, $R_k = \frac{\sqrt{3}\hbar^2}{2m_0}[-\gamma_3(k_x^2 - k_y^2) + 2i\gamma_2 k_x k_y]$, $S_k = \frac{\sqrt{3}\hbar^2\gamma_3}{2m_0}(k_x - ik_y)k_z$, $P_\epsilon = -a_v(\epsilon_{xx} + \epsilon_{yy} + \epsilon_{zz})$, $Q_\epsilon = -\frac{b}{2}(\epsilon_{xx} + \epsilon_{yy} - 2\epsilon_{zz})$, $R_\epsilon = \frac{d}{2}(\epsilon_{xx} - \epsilon_{yy}) - i\sqrt{3}b\epsilon_{xy}$, and $S_\epsilon = -\frac{d}{2}(\epsilon_{xz} - i\epsilon_{yz})$, $\vec{k} = (k_x, k_y, k_z) \equiv -i\vec{\nabla}_{\vec{r}}$ is the wave vector operator, $\vec{r} = (x, y, z)$ is the coordinate position of carrier, $e > 0 (m_0)$ stands for the elementary charge (mass) of free electron, and $\gamma_1 = 7.1$, $\gamma_2 = 2.02$, $\gamma_3 = 2.91$, $a_v = 1.16$ eV, $b = -1.7$ eV, and $d = -4.55$ eV are the Luttinger parameters for GaAs. In the numerical studies, according to the observations of atomic force microscope we model the shape of elongated GaAs/$Al_{0.35}Ga_{0.65}$As DE-QDs in terms of the characteristic function,

$$X(\vec{r}) = \begin{cases} 1, & 0 \leqslant z \leqslant H \\ 0, & \text{elsewhere,} \end{cases} \exp\left(-\frac{x^2}{\Lambda_x^2} - \frac{y^2}{\Lambda_y^2}\right) \tag{4}$$

where H is the height of QD and $\Lambda_{x/y}$ parametrize the lateral characteristic length of QD along the x/y direction [29,32]. In this work, we consider asymmetric QDs on (001)-substrate and elongated along the crystalline axis of $[1\bar{1}0]$, and specify the growth (elongation) axis as the z (x) axis. The confining potential of a GaAs/AlGaAs QD for a carrier can be written as $V^\nu_{\rm QD}(\vec{r}_\nu) = V^\nu_b \cdot X_{\rm QD}(\vec{r}_\nu)$, where $\nu = e/h$ denotes electron/hole and the band-offset $V^e_b = 300$ meV and $V^h_b = 200$ meV are taken for GaAs/AlGaAs heterostructure.

2. Single-band model for a conduction electron in a stressed QD

In the single-band model, the Schrödinger equations for a single electron in a stressed QD reads $H_e g^e_{i_e} = E^e_{i_e} g^e_{i_e}$, where

$$H_e = \frac{\hbar^2\left(k_x^2 + k_y^2 + k_z^2\right)}{2m^*_e} + V^e_{\rm QD}(\vec{r}_e) + a_c(\epsilon_{xx} + \epsilon_{yy} + \epsilon_{zz}) \tag{5}$$

is the strain-dependent Hamiltonian for single electron in the single-band model, $g^e_{i_e}$ is the envelope wave function of electron, $V^e_{\rm QD}(\vec{r}_e)$ is the position-dependent confining potential for an electron in the dot, $m^*_e = 0.067\, m_0$ is the effective mass of electron, m_0 is the free electron mass, and $a_c = -8.013$ eV for GaAs [40].

In the presence of an electric field, $\vec{F} = (F_x, F_y, _F z)$, the field-induced Hamiltonian for an electron (a valence hole), $e\vec{F} \cdot \vec{r}_e$ ($-e\vec{F} \cdot \vec{r}_h$), is imposed to Eq. (5) [Eq. (3)], where e (> 0) is the elementary charge of electron. The energy levels and wave functions of a single electron (hole) in a GaAs QD are numerically calculated within the single-band effective mass (four-band $k \cdot p$) theory using the finite-difference method as employed in Ref. [46].

3. Computations of the excitonic fine structures of QDs

Following the methodology of Ref. [46], the Hamiltonian for an interacting exciton in a QD reads $H_X = \sum_{i_e} E^e_{i_e} c^+_{i_e} c_{i_e} + \sum_{i_h} E^h_{i_h} h^+_{i_h} h_{i_h} - \sum_{i_e,j_h,k_h,l_e} V^{eh}_{i_e,j_h,k_h,l_e} c^+_{i_e} h^+_{j_h} h_{k_h} c_{l_e} + \sum_{i_e,j_h,k_h,l_e} V^{eh,xc}_{i_e,j_h,k_h,l_e} c^+_{i_e} h^+_{j_h} h_{k_h} c_{l_e}$, where i_e (i_h) represents a composite index composed of the labels of orbital and spin of a single-electron (single-hole) state, $c^+_{i_e}$ and c_{i_e} ($h^+_{i_h}$ and h_{i_h}) are the particle creation and annihilation operators,

$$V^{eh}_{i_e,j_h,k_h,l_e} \equiv \iint d^3r_e d^3r_h \psi^{e*}_{i_e}(\vec{r}_1)\psi^{h*}_{j_h}(\vec{r}_2) \times \frac{e^2}{4\pi\epsilon_0\epsilon_b|\vec{r}_{12}|}\psi^h_{k_h}(\vec{r}_2)\psi^e_{l_e}(\vec{r}_1) \tag{6}$$

are the matrix elements of Coulomb interactions causing the electron-hole scatterings, and

$$V^{eh,xc}_{i_e,j_h,k_h,l_e} \equiv \iint d^3r_1 d^3r_2 \psi^{e*}_{i_e}(\vec{r}_2)\psi^h_{j_h}(\vec{r}_2) \times \frac{e^2}{4\pi\epsilon_0\epsilon_b|\vec{r}_{12}|}\psi^{h*}_{k_h}(\vec{r}_1)\psi^e_{l_e}(\vec{r}_1) \tag{7}$$

are those of *e-h exchange* interactions, $\vec{r}_i$ denotes the coordinate position of particle, $\vec{r}_{12} \equiv \vec{r}_1 - \vec{r}_2$, ϵ_0 is vacuum permittivity, ϵ_b is the dielectric constant of QD material ($\epsilon_b = 12.9$ for GaAs), $E^e_{i_e}$ and $E^h_{i_h}$ ($\psi^e_{i_e}$ and $\psi^h_{i_h}$) are the eigenenergies (wave functions) of a single electron and single hole in the QD, respectively.

Since our interest is in the fine structures of the lowest exciton states, we take into account only the relevant lowest single-electron and single-hole orbitals and, for the brevity of notation, label them only with the spin indices, i.e., $|\psi^e_{i_e=\uparrow_e/\downarrow_e}\rangle \equiv |\uparrow_e/\downarrow_e\rangle$, ($|\psi^h_{i_h=\Uparrow'_h/\Downarrow'_h}\rangle \equiv |\Uparrow'_h/\Downarrow'_h\rangle$), where $\uparrow_e/\downarrow_e$ denotes the up/down electron spin and $\Uparrow'_h$ / $\Downarrow'_h$ indicates the up/down pseudospin of a HH-like hole state. In the reduced basis of the direct products of the single-electron and -hole states, $|\uparrow_e\rangle|\Downarrow'_h\rangle$ and $|\downarrow_e\rangle|\Uparrow'_h\rangle$, being the two lowest BX configurations, the Hamiltonian for a valence-band-mixed BX in a QD is written as a 2×2 matrix,

$$H_X = \begin{pmatrix} E^{(0)}_X & \tilde{\Delta}^{xc}_{\text{eff}} \\ \tilde{\Delta}^{xc\,*}_{\text{eff}} & E^{(0)}_X \end{pmatrix}, \tag{8}$$

where $E^{(0)}_X = E^e_{\uparrow_e} + E^h_{\Downarrow'_h} - V^{eh}_{\uparrow_e\Downarrow'_h\Downarrow'_h\uparrow_e} = E^e_{\downarrow_e} + E^h_{\Uparrow'_h} - V^{eh}_{\downarrow_e\Uparrow'_h\Uparrow'_h\downarrow_e}$ denotes the energy of exciton regardless of the $e-h$ exchange interactions, and $\tilde{\Delta}^{xc}_{\text{eff}} \equiv V^{ehxc}_{\uparrow\Downarrow'\Uparrow'\downarrow}$ is the off-diagonal matrix element of the $e-h$ exchange interaction that couples the two VBM BX configurations of opposite angular momenta and results in the FSS of the exciton doublet, $|S| = 2|\tilde{\Delta}^{xc}_{\text{eff}}|$.

In the numerical calculation, the matrix elements of *e-h* exchange interactions are divided by the short-ranged and long-ranged parts according to the averaged Wigner-Seitz radius, and computed separately [45,46]. The former is treated in the dipole-dipole interaction approximation and numerically integrated using trapezoidal rules and graphics processing unit (GPU) parallel computing technique for numerical acceleration. The latter is considered for the matrix elements involving the exciton basis of the same angular momenta and evaluated using the formalism of Eq. (2.17) in Ref. [43], in terms of the energy splitting between the BX and DX states of a QD, $E^S_X = \Delta^{xc}_{eh,\text{bulk}} \times [\pi(a^*_B)^3 \int d^3r |g^e_{s_z=\pm\frac{1}{2}}|^2 |g^h_{j_z=\mp\frac{3}{2}}|^2]$, which is extrapolated, in terms of the effective Bohr radius of exciton a^*_B, from the BX-DX splitting $\Delta^{xc}_{eh,\text{bulk}} = 20\ \mu$eV of a pure HH exciton in the GaAs bulk.

From the solved eigenstates, $|\Psi^X_\pm\rangle$, and the corresponding eigenenergies, $E^X_\pm = E^{(0)}_X \pm |\tilde{\Delta}^{xc}_{\text{eff}}|$, for Eq. (8), one can calculate the intensities $I_\pm(\hat{e}, \omega)$ of the $\hat{e}$-polarized photoluminescences (PLs) from the exciton states using the formalism of the Fermi's golden rule, as employed in Ref. [46]. The PL intensity as a function of the polarization $\hat{e}$ reaches the maximum, $I_{\pm,\max} = I_\pm(\hat{e} = \hat{e}_\pm, \omega = E^X_\pm/\hbar)$, as the polarization is along the optical axis of the exciton state $|\Psi^X_\pm\rangle$, specified by the unit vector along the axis, $\hat{e}_\pm = (\cos\phi^{\text{opt}}_\pm, \sin\phi^{\text{opt}}_\pm, 0)$. Note that both exciton basis for Eq. (8) are circularly polarized. The *e-h* exchange interaction $\tilde{\Delta}^{xc}_{\text{eff}}$ leading to the off-diagonal matrix element of Eq. (8) mixes the both circularly polarized exciton basis and the resulting eigenstates of exciton usually turn out to be linear polarized. As discussed thoroughly in Ref. [46], the exciton eigenstates of an x-elongated QD are polarized in the direction parallel or perpendicular to the elongation of the QD (along the x or y axes) as the off-diagonal matrix elements are real. On the other hand, the misaligned polarization of a exciton eigenstate from the elongation axis results from the off-diagonal matrix elements that are complex and can be characterized by a nonzero phase angle, which is related to the phase angle ϕ_β introduced previously for the HH-LH coupling of an exciton in the group theory analysis and is an indication of the lowered symmetry. As previously discussed in the group theory analysis, the lowering of the symmetry of QD makes it no longer possible to tune the FSS of an elongated QD down to zero. Thus, the feasibility of using external tuning knobs to eliminate the FSS of an elongated QD can be observed from the orientation, i.e., $\phi^{\text{opt}}_\pm$, of the optical polarization of the exciton states (see if it is aligned to or misaligned from the elongation axis). More discussion on the issue for the specific examples of QDs will be given in the next section.

III. RESULTS AND DISCUSSION

A. Useful stress actuators predicted by the group theory

1. Single uniaxial stress

As a known example, using a single uniaxial stress can fully eliminate the FSS of an elongated QD only if the stress and elongation axes are *exactly* aligned ($\phi_1 = 0°$) [17]. Substituting $\sigma_2 = 0$ into Eq. (2), we obtain $\sigma_1 \sin 2\phi_1 = 0$, indicating $\phi_1 = 0$ for $\sigma_1 \neq 0$, i.e., the perfect alignment of the stress σ_1 onto the elongation axis of QD. By contrast, with a misaligned single uniaxial stress of $\phi_1 \neq 0$, Eq. (2) is no longer fulfilled unless $\sigma_2 \neq 0$, indicating the need of the second tuning knob for retaining the C_{2v} symmetry of QD and the possibility of fully eliminating the FSS of the dot.

2. Two uniaxial stresses

For the cases of two uniaxial stresses ($\sigma_1 \neq 0, \sigma_2 \neq 0$), let us define the stress ratio by $m \equiv \frac{\sigma_2}{\sigma_1}$ and rewrite Eq. (2) as $m(\phi_1, \phi_2) = -\frac{\sin 2\phi_1}{\sin 2\phi_2}$ for further analysis. In Fig. 3, we plot the contour curves of m as a function of ϕ_1 and ϕ_2. By tracing the m-contours in Fig. 3 where Eq. (2) is surely fulfilled, we are able to predict various useful dual-stress actuators that can promisingly generate the strain remaining in the C_{2v} symmetry and enable the FSS elimination. Accordingly, one can determine the strength ratio m of a dual-stress arranged in specific axes with fixed (ϕ_1, ϕ_2) for the FSS elimination. In turn, for a stress actuator that can generate a pair of stresses with a fixed strength ratio m, Fig. 3 guides us to find the optimal arrangement of ϕ_1 and ϕ_2 for the purpose of FSS elimination.

For instance, a single uniaxial stress perfectly aligned to the elongation axis is represented by the vertical line for $m = 0$ and depicted in Fig. 3(a), which is useful to eliminate the FSS of an x-elongated QD as discussed previously. The horizontal contour line at $\phi_2 = 90°$ labeled by $m \to \infty$ in Fig. 3 indicates a single uniaxial stress ($\sigma_1 = 0, \sigma_2 \neq 0$) that is perpendicular to the elongation axis, as depicted by Fig. 3(d). In another case, the black circle at $(\phi_1, \phi_2) = (0°, 90°)$ that connects all m contour curves in Fig. 3 represents a generic

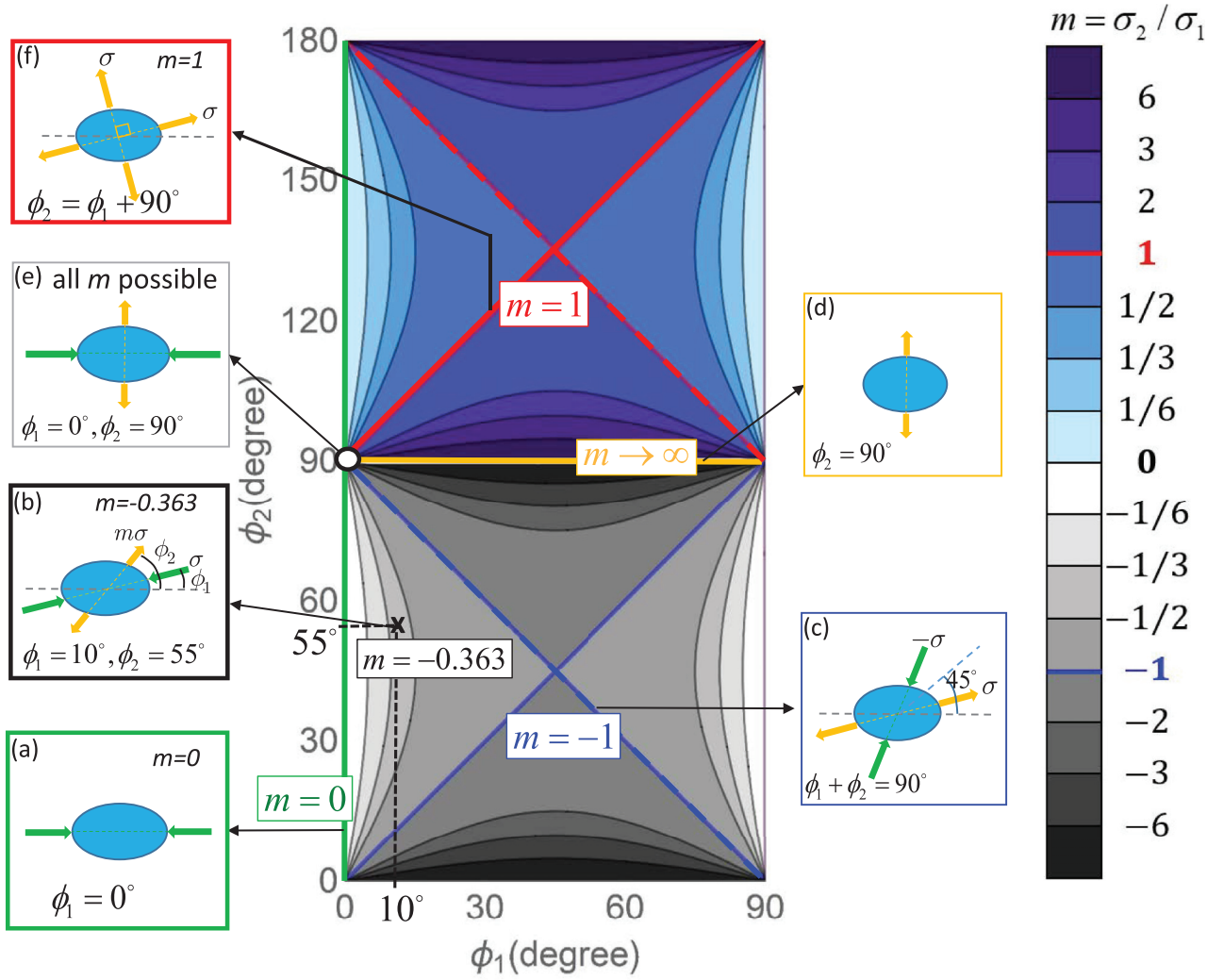

FIG. 3. The contour plot of the stress ratio $m \equiv \sigma_2/\sigma_1$ for a set of two uniaxial stresses, as a function of the angles of the stress axes, ϕ_1 and ϕ_2, that fulfills Eq.(2) and allows for the possibility of mechanically tuning and making $S = 0$. The insets depict various predicted useful dual-stress actuators that can deterministically make the FSS elimination for C_{2v} QDs.

orthogonal biaxial stress with the freely tuned σ_1 and σ_2 as depicted in Fig. 3(e). A feasible example of Fig. 3(e) is the asymmetric biaxial stress produced from the (100) facet of PMN-PT crystal, which has been successfully employed to tune and suppress the FSSs of elongated InGaAs SK-QDs, yet, with the strict requirement for the precise alignment of the stress and elongation axes [22,23].

If the σ_1-axis is misaligned from the elongation one ($\phi_1 \neq 0$), by tracing the vertical dashed line of ϕ_1 and examining the m-values of the crossed contours by the vertical line, one can find that all of the stress ratios required for FSS-elimination are nonzero, i.e., $m = \sigma_2/\sigma_1 \neq 0$. This indicates that a second tuning stress ($\sigma_2 \neq 0$) is necessary if the uniaxial stress axes cannot be aligned to the elongation one. As a specific example, for a set of two misaligned uniaxial stresses with $\phi_1 = 10^\circ$ and $\phi_2 = 55^\circ$, the stress-ratio $m = -0.363$ is predicted to suppress the FSS of a QD with the stress [see Fig. 3(b)]. The numerical confirmation for those predictions is presented in the next section.

3. Deterministic FSS-elimination with a single stress: Beyond the two-tuning-knob scheme

Beyond the use of two tuning knobs, a single knob tuning for making $S = 0$ is possible if some underlying relationship between the tuning stresses exists and can be utilized to reduce the number of independent variables of Eq. (2). Among the predicted useful dual-stress actuators, we find that a symmetric biaxial stress ($m = 1$ and $\phi_2 = \phi_1 + 90^\circ$) can act as a single mechanical tuning knob, represented by the red straight line of $m = 1$ and Fig. 3(f). Besides the equality of σ_1 and σ_2, the straightness of the $m = 1$ contour indicates the fixed angle between the σ_1 and σ_2 axes, $\Delta\phi_{21} = \phi_2 - \phi_1 = 90^\circ$, which can be naturally kept by the cubic nature of the crystal structure of PMN-PT piezoelectric crystal. Such a symmetric biaxial stress can be generated naturally from the (001) facet of PMN-PT crystal under a *single* tuning electrical bias [36,37] and remain invariant in the symmetry no matter how orientated the PMN-PT crystal is.

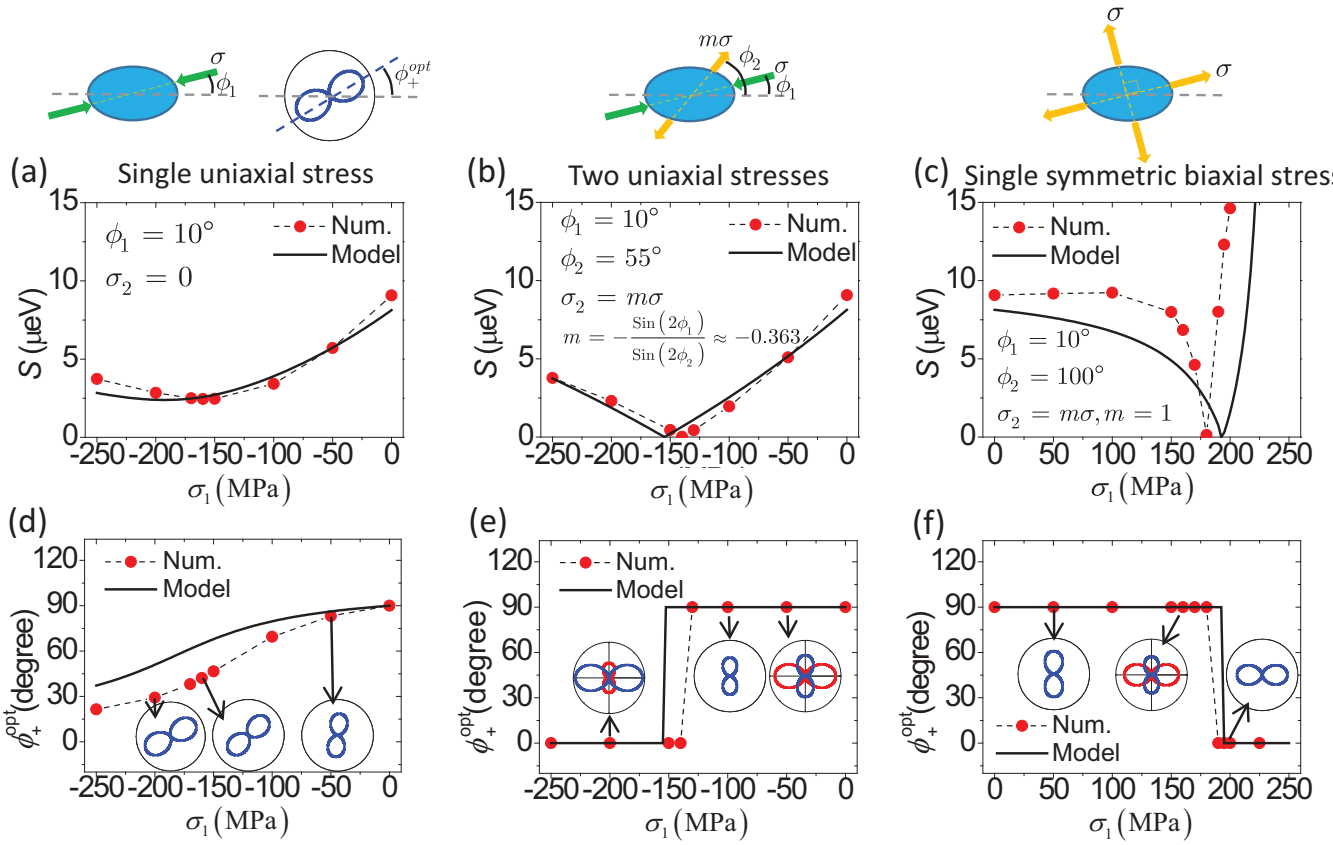

FIG. 4. The calculated fine structure splitting of the exciton doublet of a GaAs DE-QD under (a) a uniaxial stress misaligned to the elongation axis by the angle $\phi_1 = 10°$, (b) a set of two uniaxial stresses with $\phi_1 = 10°$, $\phi_2 = 55°$, and the fixed stress ratio $m = \sigma_2/\sigma_1 = \sin 2\phi_2 / \sin 2\phi_1 = -0.363$, and (c) a single symmetric biaxial stress. The numerical (model calculated) results are indicated by filled red circles (solid lines). (d)–(f): The angles, ϕ_+^{opt}, with respect to the QD-elongation axis, of the optical polarization axes of the upper level state of the exciton doublet of the QD versus the applied stresses. Insets: the polar plots of the intensities of the emitted polarized photons from the exciton doublet (blue: the upper level; red: the lower one) of the stressed QD with some specific stresses. In the numerical computation, we consider the x-elongated droplet epitaxial GaAs/AlGaAs quantum dot of $\Lambda_x = 25.7$ nm, $\Lambda_x = 17.2$ nm, and $H = 12$ nm. For the model calculation, the length parameters for the spatial extents of the wave function, $l_x = 7.9$ nm, $l_y = 6.7$ nm and $l_z = 4.3$ nm, are taken.

B. Numerical results

1. Single uniaxial stress

Figure 4(a) shows the numerically calculated FSS (S) between the lowest BX states of the x-elongated GaAs DE-QD of $H = 12$ nm, $\Lambda_x = 26$ nm, and $\Lambda_y = 17$ nm under a single tuning uniaxial stress along the direction with the angle $\phi_1 = 10°$ with respect to the x axis. As we expected, the application of the misaligned uniaxial stress leads to the reduction of the symmetry of the QD down to C_1 and cannot fully eliminate the FSS [16,17,23]. To retain the C_{2v} symmetry of QD, one can introduce and use a second tuning knob.

2. Two uniaxial stresses

Figure 4(b) shows the calculated FSS of the same stressed QD with, additionally, a second uniaxial stress set in the fixed direction with $\phi_2 = 55°$. The FSS of the QD tuned by the two mechanical knobs is shown fully eliminated with $\sigma_1 = -140$ MPa and $\sigma_2 = 51$ MPa, whose ratio $m = \frac{\sigma_2}{\sigma_1} = -0.363$ is exactly as predicted by Eq. (2). Intuitively, the necessity of using two tuning knobs to make FSS elimination is widely understood from the observed correlation between the FSS and the optical anisotropy featured by the degree as well as orientation of polarization [9,18,22,23,33], as evidenced here by the comparison between Figs. 4(a)–4(c) and Figs. 4(d)–4(f). Figures 4(d)–4(f) present the calculated angles, ϕ_+^{opt}, of the optical axes for the upper exciton level of the QD under the different types of stresses, corresponding to Figs. 4(a)–4(c), respectively. Note that, once the FSS of a QD can be tuned to be zero [see Figs. 4(b), 4(c), 4(e), and 4(f)], the orientation of optical polarization remains unchanged against the stress tuning (except that $S = 0$ happens). The angle invariance of the optical polarization implies the preservation of the C_{2v} symmetry of QD. From the above observations, the use of two tuning knobs is effective to tune the FSS and simultaneously keep the orientation of polarization invariant [9].

3. Deterministic FSS elimination with a single stress

Figure 4(c) shows the numerically calculated results for the x-elongated QD under a *single* symmetric biaxial stress with the misaligned axes from the x and y axes by $\phi_1 = \phi_2 - 90° = 10°$. As predicted by previous analysis, the numerical simulation confirms that the excitonic FSS of the C_{2v} QD

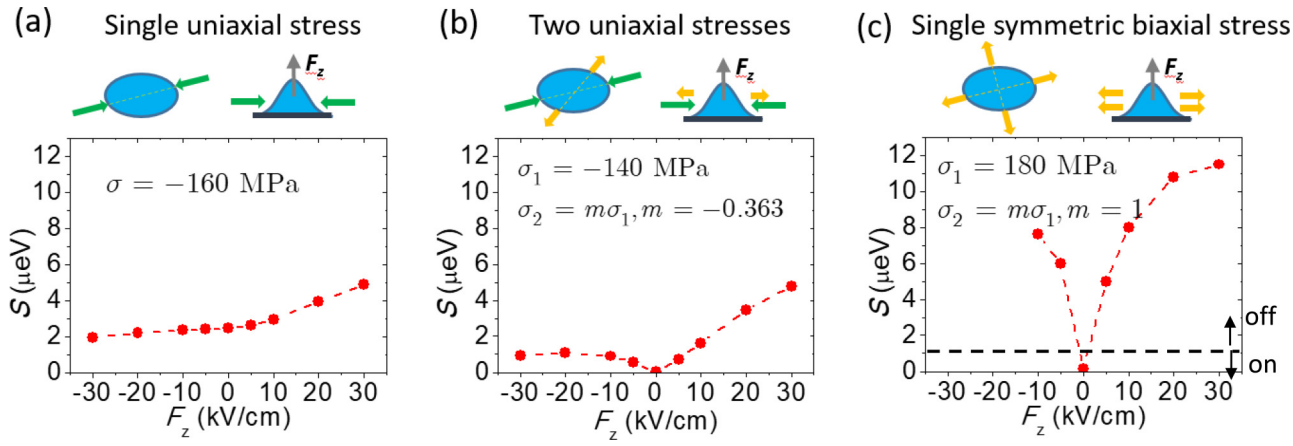

FIG. 5. Calculated excitonic fine structure splittings of the same QD under the stresses considered in Fig. 2 of the main paper, and additionally biased by a vertical electrical field, F_z. As compared with the cases of single uni-axial stress in (a) and of the dual uniaxial stress in (b), the FSS of the QD controlled by a single symmetric biaxial stress shown in (c) is most tunable by electric field, and suited to be the "on-demand" electrically triggered EPPE device, which requires the FSS to be electrically switchable below or above the threshold, $S = 1$ μeV, for the generation of entangled photon pairs.

indeed can be eliminated fully by the *single* tuning biaxial stress of $\sigma = 177$ MPa, in spite of the misalignment of the stress and elongation axes. This result examples that, beyond common intuitive understanding, the use of two tuning knobs is a sufficient but not always a necessary condition for eliminating the FSS of a QD. The full elimination of the FSS of the DE-QD with the single mechanical tuning knob is achieved by taking the advantage of the compatibility of crystal symmetry between the QD and piezoelectric actuator materials, which can always ensure the C_{2v} preservation and allow for some accidental degeneracy happening in the BX doublet. The use of a *symmetric* biaxial stress for tuning the FSSs of self-assembled QDs has been previously explored but was not found so advantageous in the FSS elimination for the studied InGaAs SK-QDs [18]. The usefulness of symmetric biaxial stress is limited for elongated InGaAs SK-QDs since there exist intrinsic strains in the SK-QDs, which are themselves *asymmetric* and spoil the symmetry of the applied biaxial stresses [18].

4. Electrical tunabilities of stressed QDs

The high tunability for the FSSs of QDs is a crucial functional feature for realizing the "on-demand" QD-based EPPEs that requires the efficient switch-on ($S < 1$ μeV) and -off ($S \gg 1$ μeV) of the devices by electrically gating for the integrated application with microelectronics. Figure 5 presents the numerically calculated excitonic FSSs of the stressed QD as considered in Figs. 4(a)–4(c) and additionally applied by a vertical electrical field, $\vec{F} = (0, 0, F_z)$. As the FSS of the QD is tuned to be nearly vanishing by an appropriate stress, an external electric field is used here to reopen the splitting to switch off the device. In turn, the device can be switched on by turning off the applied electric field. The FSS of the QD under the three types of stress control is shown all electrically tunable, but to different extents. Among them, only the FSS of the QD imposed by a single symmetric biaxial stress [Fig. 5(c)] is so well tunable by the external electric field that the FSS can be varied over a practically useful wide range of energy. In Fig. 4(c), the FSS of the stressed QD is shown quickly changed from $S = 0$ to over 5 μeV by applying the small electric field $F_z \sim 5$ kV/cm onto the QD. This is attributed to the nonlinear nature of the biaxial term (that will be discussed more by the model analysis later) in the VBM of an exciton confined in the stressed QD, which can make more impact on the VBM-relevant FSS of the QD as the wave function extents are varied only slightly by an external electric field.

IV. EFFECTIVE EXCITON MODEL

Following the methodology in Ref. [46], we proceed to establish a simplified generic exciton model for stress-controlled QDs that is consistent with the previous analysis and numerical results, and allows for more physical analysis. By treating the HH-LH coupling terms in the four-band theory as perturbation, one can derive an effective exciton Hamiltonian in the compact form of 2×2 matrix, explicitly in terms of the QD parameters and applied stresses, as presented below.

In the lowest-order approximation, the lowest spin-up (spin-down) HH-like hole state, $|\Uparrow'_h\rangle$ ($|\Downarrow'_h\rangle$), of a stressed QD can be written as $|\Uparrow'_h\rangle \approx |\Uparrow_h\rangle - \tilde{\beta}_{\rm HL}|\downarrow_h\rangle$ ($|\Downarrow'_h\rangle \approx |\Downarrow_h\rangle - \tilde{\beta}^*_{\rm HL}|\uparrow_h\rangle$), composed of the dominant pure HH component, $|\Uparrow_h\rangle$ ($|\Downarrow_h\rangle$) mixed by the secondary LH one, $|\uparrow_h\rangle$ ($|\downarrow_h\rangle$), via the complex coefficient, $\tilde{\beta}_{\rm HL} \equiv \beta_{\rm HL} e^{-i\phi_\beta}$ that reflects the degree of VBM [48]. In the parabolic model, the envelope wave function of the HH component is modeled by $\langle\vec{r}|\Uparrow'_h\rangle \equiv \psi_{\Uparrow'_h}(\vec{r}) \approx \phi_0(\vec{r})u_{j_z=3/2}(\vec{r}) - \beta^*_{\rm HL}\phi_0(\vec{r})u_{j_z=-1/2}(\vec{r})$, where $\phi_0(\vec{r}) = \sqrt{\frac{1}{\pi^{3/2} l_x l_y l_z}} \exp\{-\frac{1}{2}[(\frac{x}{l_x})^2 + (\frac{y}{l_y})^2 + (\frac{z}{l_z})^2]\}$ is the wave function of the lowest Fock-Darwin state in the parabolic model and $l_{\alpha=x,y,z}$ is the characteristic length of the wave function extent along the α direction. In the basis of the VBM-exciton configurations, $\frac{1}{\sqrt{2}}(|\downarrow_e \Uparrow'_h\rangle \pm |\uparrow_e \Downarrow'_h\rangle$, one can derive the effective exciton Hamiltonian for a stressed QD as

$$H'_X = \begin{pmatrix} E_X^{(0)} + \Re[\tilde{\Delta}_{\rm eff}] & \Im[\tilde{\Delta}_{\rm eff}] \\ -\Im[\tilde{\Delta}_{\rm eff}] & E_X^{(0)} - \Re[\tilde{\Delta}_{\rm eff}] \end{pmatrix}, \quad (9)$$

where $E_X^{(0)}$ denotes the average energy of the spin-split exciton levels, and $\tilde{\Delta}_{\rm eff}$ is the complex matrix element of the *e-h* exchange interaction between the two VBM-exciton configurations, $|\downarrow_e \Uparrow_h'\rangle$ and $|\uparrow_e \Downarrow_h'\rangle$, which, following Ref. [46], can be formulated as

$$\tilde{\Delta}_{\rm eff} = -\Delta_1 + \frac{2}{\sqrt{3}} E_X^S \cdot \tilde{\beta}_{\rm HL} \tag{10}$$

where $-\Delta_1$ is the matrix element of the attractive long-ranged *e-h* exchange interaction between the pure-HH exciton, $|\downarrow_e \Uparrow_h\rangle$ and $|\uparrow_e \Downarrow_h\rangle$, the second term on the right-hand side originates from the short-ranged *e-h exchange* interaction associated with the VBM, $\tilde{\beta}_{\rm HL}$, and E_X^S is the exchange splitting between the BX and DX states of the QD that, as an empirical parameter, can be extrapolated from the measured BX-DX splitting of GaAs bulk, $E_S^{X,\rm bulk} = 20\ \mu$eV for GaAs [46]. As a result, the FSS of exciton is given by

$$S = 2\sqrt{(\Im[\tilde{\Delta}_{\rm eff}])^2 + (\Re[\tilde{\Delta}_{\rm eff}])^2} \tag{11}$$

From the solved eigenstates of Eq. (9), the polarized PL can be calculated using the formalisms based on the Feri's golden rules as presented in Ref. [46]. For a QD with two uniaxial stresses, the VBM coefficient is derived as

$$\tilde{\beta}_{\rm HL} = \frac{\rho_{\rm HL}^0 + \lambda(\sigma_1 e^{2i\phi_1} + \sigma_2 e^{2i\phi_2})}{\Delta_{\rm HL}^0 + \mu\sigma_b}, \tag{12}$$

where $\sigma_b \equiv \sigma_1 + \sigma_2$ is the biaxial stress, $\rho_{\rm HL}^0$ ($\Delta_{\rm HL}^0$) is the matrix element of HH-LH coupling (energy difference between the pure HH and LH levels) in the absence of strain, and the constants, λ and μ, are associated with the deformation parameters of QD. Equation (11) shows that $S = 0$ requires that the both of real and imaginary parts of the exchange interaction vanish, i.e., $\Im[\tilde{\Delta}_{\rm eff}] = 0$ and $\Re[\tilde{\Delta}_{\rm eff}] = 0$. From Eqs. (10) and (12), the former condition, $\Im[\tilde{\Delta}_{\rm eff}] = 0 \propto \Im[\tilde{\beta}_{\rm HL}] = 0$ leads to that $\tilde{\beta}_{\rm HL}$ is real and $\sigma_1 \sin 2\phi_1 + \sigma_2 \sin 2\phi_2 = 0$, the same as Eq. (2) derived by the group theory.

Advantageous effects of a symmetric biaxial stress: The model analysis

With the proper consideration of the strain-dependent VBM on the base of the four-band theory, in Eq. (12) the VBM (parametrized by $\tilde{\beta}_{\rm HL}$) in a QD-confined exciton is shown tunable by uniaxial stresses or a biaxial one, so are the FSS (S) according to Eqs. (10) and (11). In Eq. (12), one sees that the terms of uniaxial stress appear in the numerator and are associated with the orientations of the stress axes (ϕ_1 and ϕ_2). In contrast, that of biaxial stress lying in the denominator is shown irrelevant to the orientation angles of the applied uniaxial stresses. This implies that tuning the FSS of a QD with a single biaxial stress could be free from uncertainty in the poor-controlled alignment of the stress and elongation axes, while the orientation alignment of uniaxial stress and elongation axes is critical for the FSS tuning.

For the comparison with the numerical results in Fig. 4, the FSSs and the optical polarizations of the stressed QD are calculated by using the exciton model with the length parameters of the wave function, $l_x = 7.9$ nm, $l_y = 6.7$ nm, and $l_z = 4.3$ nm, as presented by the black solid lines in Fig. 4, showing the consistence with the numerical results. Our derived exciton model is consistent with and even beyond the previous one in Ref. [49] that was developed for their studies of strained InGaAs/AlGaAs SK-QDs. In the latter model, the matrix elements of the exciton Hamiltonian were assumed to be linearized with respect to the applied stress and the biaxial term in the denominator of Eq. (12) was overlooked. The assumption of linear stress dependence is acceptable for the studied InGaAs/AlGaAs SK-QDs where the intrinsic biaxial strain from the lattice mismatch between InGaAs and AlGaAs is significant so that $\Delta_{\rm HL}^0 \gg \mu\sigma_b$ and the effect of external biaxial stress, σ_b, is thus negligible. For unstrained GaAs DE-QDs under our study, $\Delta_{\rm HL}^0$ is small because of the absence of intrinsic biaxial strain and the application of an external biaxial stress makes more impaction onto the electronic and excitonic structures. Expanding Eq. (12) in terms of stress, an external biaxial stress lying in the denominator yields considerable high-order stress terms, making the FSSs of DE-QDs sensitive to and well tunable by external stresses as shown in Fig. 4(c). For the same sake, the nonlinear nature

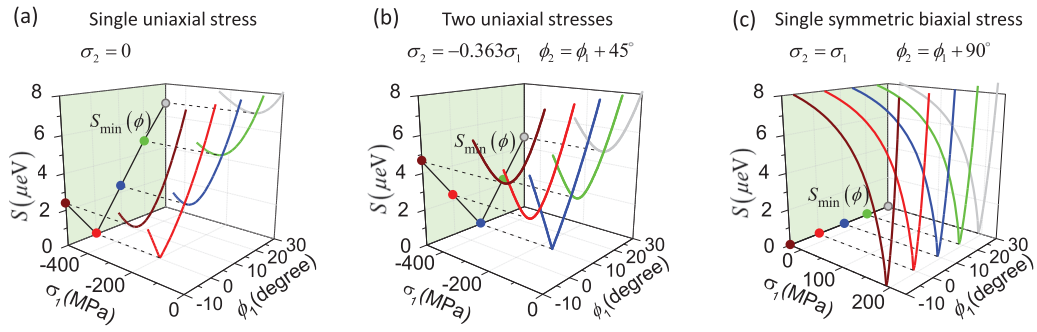

FIG. 6. Calculated excitonic fine structure splittings of the same QD considered in Fig. 2 with (a) a single uniaxial stress, (b) a set of two uniaxial stresses, and (c) a single symmetric biaxial stress, versus the varied stress σ_1 from the actuators arranged in varied orientation, ϕ_1 (while m and $\Delta\phi_{12} = \phi_2 - \phi_1$ are kept fixed). The minimal stress-tuned fine structure splittings ($S_{\rm min}$) of the stressed QD versus ϕ_1 are plotted in the x-z plane of the plots. One sees that, with a single uniaxial stress or the combination of two independently tunable uniaxial stresses, the S can be zero only as ϕ_1 is at a specific angle. By contrast, with a symmetric biaxial stress, the S of the stressed QD can be tuned to be stably zero against any variation of ϕ_1.

of the biaxial term in the denominator of Eq. (12) for the VBM of exciton leads to the high electrical tunability of the FSS of the QD with a biaxial stress, as presented in Fig. 5. Figure 4(c) reveals the pronounced effect of biaxial stress on the high tunability (maximally ∼600 μeV/GPa) for the FSS of the QD, which might be related to the stress-enhanced supercoupling in the VBM of exciton as recently reported by Ref. [38].

Figure 6 shows the calculated FSS, S, of the stressed QD versus the stresses generated from the micromachined PMN-PT actuators of Fig. 4 but arranged in various orientations. The minimum stress-tuned FSSs, $S_{\min}$, of the stressed QD versus the varied orientations of the stress actuators are projected onto the $x-z$ plane of Fig. 6. Figures 6(a) and 6(b) show that it is very critical to set the orientations of a single uniaxial stress or a set of two asymmetric uniaxial ones so as to fully eliminate the FSS of the stressed QD. With the application of the single uniaxial stress (the set of two uniaxial stresses), S can be fully vanishing only as the orientation of the stress of σ_1 is set exactly to be $\phi_1 = 0^\circ$ ($\phi_1 = 10^\circ$). By contrast, the $S_{\min}$ of a QD can be eliminated always by a tuning symmetric biaxial stress, disregarding any orientation variation of the biaxial stress actuator, as shown in Fig. 6(c). It is the phase irrelevance of the biaxial stress term in the denominator of Eq. (12) that makes the robustness of the FSS tuning against the variation of actuator orientation.

V. CONCLUSION

In summary, we present a theoretical and computational investigation of the excitonic FSSs of GaAs/AlGaAs DE-QDs mechanically tuned by the stress actuators of micromachined PMN-PT crystals. From group theory analysis confirmed by fully numerical simulation, we reveal the general principle for the optimal arrangement of two uniaxial stresses whose application onto elongated an elongated GaAs DE-QD can certainly eliminate the FSS of an exciton therein. Moreover, as a main finding of this work, we point out that the use of two tuning knobs for a certain elimination of the FSSs of QDs is a sufficient but not always a necessary condition as commonly believed. The feasibility of using only single knob for making QD-based EPPE devices is significant to simplify the process of device fabrication and allows for developing versatile photonic devices crucial in integrated photonic systems. As a feasible example, a *single* symmetric biaxial stress naturally generated from the (001) PMN-PT actuator can be a single tuning knob for eliminating the FSSs of DE-QDs, whose feasibility is achieved by taking the advantage of the compatibility of the crystal structure symmetries of the QD and piezoelectric materials. Beyond the existing exciton models for stress-tuned QDs, our derived effective exciton model on the base of multiband theory well captures the nonlinearity nature of biaxial stress terms in the exciton Hamiltonian and enables us to understand more the usefulness of symmetric biaxial stress, including the robustness of deterministic FSS elimination against the poor-controlled orientations of stress actuators and the high electrical and mechanical FSS tunability crucial for realizing "on-demand" electrically triggered EPPEs.

ACKNOWLEDGMENTS

The paper is supported by the Ministry of Science and Technology, Taiwan, under Contracts No. MOST-106-2112-M-009-015-MY3, No. MOST-106-2221-E-009-113-MY3, and No. MOST-107-2633-E-009-003, and by National Center for High-Performance Computing (NCHC), Taiwan.

[1] R. Horodecki, P. Horodecki, M. Horodecki, and K. Horodecki, Rev. Mod. Phys. **81**, 865 (2009).
[2] O. Benson, C. Santori, M. Pelton, and Y. Yamamoto, Phys. Rev. Lett. **84**, 2513 (2000).
[3] M. Müller, S. Bounouar, K. D. Jöns, M. Glässl, and P. Michler, Nat. Photon. **8**, 224 (2014).
[4] R. J. Young, R. M. Stevenson, P. Atkinson, K. Cooper, D. A. Ritchie, and A. J. Shields, New. J. Phys. **8**, 29 (2006).
[5] N. Akopian, N. H. Lindner, E. Poem, Y. Berlatzky, J. Avron, D. Gershoni, B. D. Gerardot, and P. M. Petroff, Phys. Rev. Lett. **96**, 130501 (2006).
[6] L. He, M. Gong, C.-F. Li, G.-C. Guo, and A. Zunger, Phys. Rev. Lett. **101**, 157405 (2008).
[7] A. J. Bennett, M. A. Pooley, R. M. Stevenson, M. B. Ward, R. B. Patel, A. B. de La Giroday, N. Sköld, I. Farrer, C. A. Nicoll, D. A. Ritchie *et al.*, Nat. Phys. **6**, 947 (2010).
[8] A. Mohan, M. Felici, P. Gallo, B. Dwir, A. Rudra, J. Faist, and E. Kapon, Nat. Photon. **4**, 302 (2010).
[9] R. Trotta, E. Zallo, C. Ortix, P. Atkinson, J. D. Plumhof, J. van den Brink, A. Rastelli, and O. G. Schmidt, Phys. Rev. Lett. **109**, 147401 (2012).
[10] T. Kuroda, T. Mano, N. Ha, H. Nakajima, H. Kumano, B. Urbaszek, M. Jo, M. Abbarchi, Y. Sakuma, K. Sakoda *et al.*, Phys. Rev. B **88**, 041306 (2013).
[11] K. Kowalik, O. Krebs, A. Lemaitre, S. Laurent, P. Senellart, P. Voisin, and J. A. Gaj, Appl. Phys. Lett. **86**, 041907 (2005).
[12] K. Kowalik, O. Krebs, A. Lemaître, B. Eble, A. Kudelski, P. Voisin, S. Seidl, and J. A. Gaj, Appl. Phys. Lett. **91**, 183104 (2007).
[13] R. M. Stevenson, R. J. Young, P. See, D. G. Gevaux, K. Cooper, P. Atkinson, I. Farrer, D. A. Ritchie, and A. J. Shields, Phys. Rev. B **73**, 033306 (2006).
[14] C. H. Lin, W. T. You, H. Y. Chou, S. J. Cheng, S. D. Lin, and W. H. Chang, Phys. Rev. B **83**, 075317 (2011).
[15] A. Muller, W. Fang, J. Lawall, and G. S. Solomon, Phys. Rev. Lett. **103**, 217402 (2009).
[16] S. Seidl, M. Kroner, A. Högele, K. Karrai, R. J. Warburton, A. Badolato, and P. M. Petroff, Appl. Phys. Lett. **88**, 203113 (2006).
[17] R. Singh and G. Bester, Phys. Rev. Lett. **104**, 196803 (2010).
[18] J. Wang, M. Gong, G.-C. Guo, and L. He, Appl. Phys. Lett. **101**, 063114 (2012).
[19] M. A. Pooley, A. J. Bennett, R. M. Stevenson, A. J. Shields, I. Farrer, and D. A. Ritchie, Phys. Rev. Appl. **1**, 024002 (2014).
[20] R. Trotta, J. Martín-Sánchez, J. S. Wildmann, G. Piredda, M. Reindl, C. Schimpf, E. Zallo, S. Stroj, J. Edlinger, and A. Rastelli, Nat. Commun. **7**, 10375 (2016).

[21] R. Trotta, J. Martín-Sánchez, I. Daruka, C. Ortix, and A. Rastelli, Phys. Rev. Lett. **114**, 150502 (2015).
[22] Y. Chen, J. Zhang, M. Zopf, K. Jung, Y. Zhang, R. Keil, F. Ding, and O. G. Schmidt, Nat. Commun. **7**, 10387 (2016).
[23] J. Zhang, J. S. Wildmann, F. Ding, R. Trotta, Y. Huo, E. Zallo, D. Huber, A. Rastelli, and O. G. Schmidt, Nat. Commun. **6**, 10067 (2015).
[24] N. Koguchi, S. Takahashi, and T. Chikyow, J. Cryst. Growth **111**, 688 (1991).
[25] K. Watanabe, N. Koguchi, and Y. Gotoh, Jpn. J. Appl. Phys. **39**, L79 (2000).
[26] S. Kumar, E. Zallo, Y. H. Liao, P. Y. Lin, R. Trotta, P. Atkinson, J. D. Plumhof, F. Ding, B. D. Gerardot, S. J. Cheng *et al.*, Phys. Rev. B **89**, 115309 (2014).
[27] D. Bimberg and U. W. Pohl, Mater. Today **14**, 388 (2011).
[28] *Single Semiconductor Quantum Dots*, edited by P. Michler (Springer-Verlag, Berlin, 2009).
[29] Y. H. Liao, C. C. Liao, C. H. Ku, Y. C. Chang, S. J. Cheng, M. Jo, T. Kuroda, T. Mano, M. Abbarchi, and K. Sakoda, Phys. Rev. B **86**, 115323 (2012).
[30] D. Huber, M. Reindl, Y. Huo, H. Huang, J. S. Wildmann, O. G. Schmidt, A. Rastelli, and R. Trotta, Nat. Commun. **8**, 15506 (2017).
[31] T. E. Schlesinger and T. Kuech, Appl. Phys. Lett. **49**, 519 (1986).
[32] J. G. Keizer, B. J., P. M. Koenraad, T. Mano, T. Noda, and K. Sakoda, Appl. Phys. Lett. **96**, 062101 (2010).
[33] J. D. Plumhof, V. Křápek, F. Ding, K. D. Jöns, R. Hafenbrak, P. Klenovský, A. Herklotz, K. Dörr, P. Michler, A. Rastelli *et al.*, Phys. Rev. B **83**, 121302 (2011).
[34] S. Kumar, R. Trotta, E. Zallo, J. D. Plumhof, P. Atkinson, A. Rastelli, and O. G. Schmidt, Appl. Phys. Lett. **99**, 161118 (2011).
[35] J. Martín-Sánchez, R. Trotta, A. Mariscal, R. Serna, G. Piredda, S. Stroj, J. Edlinger, C. Schimpf, J. Aberl, T. Lettner *et al.*, Semicond. Sci. Technol. **33**, 013001 (2017).
[36] Z. Wu, Y. Zhang, G. Bai, W. Tang, J. Gao, and J. Hao, Opt. Express **22**, 29014 (2014).
[37] S. Heo, C. Oh, M. J. Eom, J. S. Kim, J. Ryu, J. Son, and H. M. Jang, Sci. Rep. **6**, 22228 (2016).
[38] J. W. Luo, G. Bester, and A. Zunger, Phys. Rev. B **92**, 165301 (2015).
[39] See Supplemental Material at http://link.aps.org/supplemental/10.1103/PhysRevB.98.155315 for the technical details in the analysis of group theory, the derivation of the strain tensors, and the model analysis for the fine structures of exciton.
[40] S. L. Chuang, *Physics of Photonic Devices,* 2nd ed. (Wiley, New Jersey, 2009).
[41] J. F. Nye, *Physical Properties of Crystals* (Clarendon Press, Oxford, 1960).
[42] H. J. Weber and G. B. Arfken, *Essential Mathematical Methods for Physicists* (Elsevier Academic Press, Amsterdam, 2004).
[43] T. Takagahara, Phys. Rev. B **62**, 16840 (2000).
[44] E. L. Ivchenko, *Optical Spectroscopy of Semiconductor Nanostructures* (Alpha Science International, Ltd., Harrow, UK, 2005).
[45] E. Kadantsev and P. Hawrylak, Phys. Rev. B **81**, 045311 (2010).
[46] S.-J. Cheng, Y.-H. Liao, and P.-Y. Lin, Phys. Rev. B **91**, 115310 (2015).
[47] Y.-N. Wu, M.-F. Wu, Y.-W. Ou, Y.-L. Chou, and S.-J. Cheng, Phys. Rev. B **96**, 085309 (2017).
[48] Y. Léger, L. Besombes, L. Maingault, and H. Mariette, Phys. Rev. B **76**, 045331 (2007).
[49] M. Gong, W. Zhang, G. C. Guo, and L. He, Phys. Rev. Lett. **106**, 227401 (2011).